Cell Biology International ISSN 1065-6995
doi: 10.1002/cbin.11335

RESEARCH ARTICLE

Hypoxia-induced apoptosis of astrocytes is mediated by reduction of Dicer and activation of caspase-1

Yeo Wool Kang[1], Yoon Suk Kim[2], Jun Young Park[3], Ga-eul Chu[1], Young Chul Yang[1], Byung Young Choi[1] and Won Gil Cho[1]*

1 Department of Anatomy, Yonsei University Wonju Medical College, 20, Ilsan-ro, Wonju-si, Gangwon-do, 26426, Korea
2 Department of Biomedical Laboratory Science, College of Health Sciences, Yonsei University—Mirae Campus, 1 yonseidae-gil, Wonju, Gangwon-do, 26493, Korea
3 Department of Nuclear Medicine, Severance Hospital, Yonsei University College of Medicine, 50-1 Yonsei-ro, Seodaemun-gu, Seoul, 03722, Korea

Abstract

Hypoxia is a condition in which the whole body or a region of the body is deprived of oxygen supply. The brain is very sensitive to the lack of oxygen and cerebral hypoxia can rapidly cause severe brain damage. Astrocytes are essential for the survival and function of neurons. Therefore, protecting astrocytes against cell death is one of the main therapeutic strategies for treating hypoxia. Hence, the mechanism of hypoxia-induced astrocytic cell death should be fully elucidated. In this study, astrocytes were exposed to hypoxic conditions using a hypoxia work station or the hypoxia mimetic agent cobalt chloride ($CoCl_2$). Both the hypoxic gas mixture (1% O_2) and chemical hypoxia-induced apoptotic cell death in T98G glioblastoma cells and mouse primary astrocytes. Reactive oxygen species were generated in response to the hypoxia-mediated activation of caspase-1. Active caspase-1 induced the classical caspase-dependent apoptosis of astrocytes. In addition, the microRNA processing enzyme Dicer was cleaved by caspase-3 during hypoxia. Knockdown of Dicer using antisense oligonucleotides induced apoptosis of T98G cells. Taken together, these results suggest that astrocytic cell death during hypoxia is mediated by the reactive oxygen species/caspase-1/classical caspase-dependent apoptotic pathway. In addition, the decrease in Dicer levels by active caspase-3 amplifies this apoptotic pathway via a positive feedback loop. These findings may provide a new target for therapeutic interventions in cerebral hypoxia.

Keywords: apoptosis; brain/nervous system; neurodegeneration; oxidative stress

Introduction

The blockage of cerebral blood flow results in a shortage of oxygen supply to the affected area (Prabhakar, 2001). Low oxygen concentrations limit the generation of adenosine triphosphate (ATP) by aerobic respiration and ATP depletion causes irreversible damage to cells (Wheaton and Chandel, 2010). In the core of the ischemic region, irreversible, severe tissue damage occurs within minutes after a reduction in blood flow. However, in the region surrounding the ischemic core, neurons experience secondary tissue damage, such as inflammation and apoptosis (Sendoel and Hengartner, 2014).

Astrocytes are the most abundant glial cells in the central nervous system (CNS) (Sofroniew and Vinters, 2010). They are essential for the survival and function of neurons. After CNS injury, astrocytes release cytokines and growth factors that promote the growth of axons and dendrites of healthy neurons in the damaged area. During hypoxia, astrocytes secrete vascular endothelial growth factor (VEGF) to increase neuron survival (Jin et al., 2002). Although astrocytes are considered to be more insult-resistant than neuron, ischemia (Giffard and Swanson, 2005), alcohol intoxication (Vallés et al., 2004), and carbon monoxide intoxication (Vieira et al., 2015) can damage astrocytes. In such conditions, the disruption of astrocytes has devastating effects on neuronal integrity.

Dicer is an RNase III ribonuclease that processes a double-stranded RNA (dsRNA) substrate into 21–24 nucleotide long sequences (MacRae et al., 2006). Dicer processes long dsRNA molecules to generate the functional short interfering RNAs

*Corresponding author: e-mail: wch01@yonsei.ac.kr

Abbreviations: AMD, age-related macular degeneration; ASO, antisense oligonucleotide; ATP, adenosine triphosphate; CNS, central nervous system; DCFDA, 2′,7′-dichlorofluorescin diacetate; dsRNA, double-stranded RNA; HIF1- α, hypoxia inducible factor-1α; NAC, *N*-acetyl-cysteine; PARP, poly(ADP-ribose) polymerase; ROS, reactive oxygen species; tDicer, truncated Dicer; VEGF, vascular endothelial growth factor

of the RNA interference pathway (Ge et al., 2014). Its ability to process dsRNA substrates is also required for microRNA (miRNA) maturation. Dicer cleaves off the loop from pre-miRNAs to produce mature miRNAs in the cytoplasm (MacFarlane and Murphy, 2010). Dysregulation of Dicer is observed in various types of cancer and is associated with miRNA dysregulation. In many cases, the expression level of Dicer is downregulated, which induces the proliferation, migration, and invasion of tumor cells (Kumar et al., 2009). Apart from cancer, downregulation of Dicer has also been observed in age-related macular degeneration (AMD), a leading cause of blindness. In AMD, the downregulation of Dicer-mediated retinal pigmented epithelial cell death has been observed (Ambati and Fowler, 2012).

Protecting astrocytes from cell death is one therapeutic strategy for limiting and reducing damage to the CNS caused by hypoxia (Zhao and Rempe, 2010). In the present study, we report that the hypoxia-induced apoptosis of astrocytes is mediated by a decrease in RNase III ribonuclease Dicer levels via caspase-1 activation. Moreover, we suggest that Dicer may be a new target for therapeutic interventions in cerebral hypoxia.

Materials and methods

Cells and animals

The T98G human glioblastoma cell line was purchased from the ATCC (CRL-1690™; Manassas, VA, USA). The cells were grown in Dulbecco's modified Eagle's medium (DMEM) supplemented with 10% fetal bovine serum (FBS), streptomycin (50 μg/mL), and penicillin (50 U/mL; GIBCO/BRL Life Technologies, Carlsbad, CA, USA) and maintained at 37°C in a humidified atmosphere with 5% CO_2. Mouse pups derived from female BABL/c mice were used as the donors of the primary astrocyte culture. All animal housing, handling, and experimental procedures were approved by the Institutional Animal Care and Use Committee (IACUC) of Yonsei University at Wonju College of Medicine (IACUC approval no.YWC-190110-1) and performed in accordance with the Animal Care and Use Guidelines of Yonsei University at Wonju College of Medicine. Hypoxic cells were grown in a humidified Whitley H35 Hypoxystation (Don Whitley Scientific Ltd., Shipley, UK) at 37°C, with 1% O_2 and 5% CO_2. Chemical hypoxia was induced using the hypoxia-mimicking agent cobalt chloride ($CoCl_2$), which mimics the consequence of hypoxia by causing the accumulation of hypoxia inducible factor-1α (HIF-1α) (Salceda and Caro, 1997).

Primary culture of mouse astrocytes

Mixed cortical cells were isolated from P1 to P4 mouse pups (BALB/c) for astrocyte cultures (Schildge et al., 2013). The brain was removed and placed in a dissecting dish filled with ice-cold Hank's balanced salt solution (HBSS) (GIBCO/BRL Life Technologies). Under a surgical microscope (Carl Zeiss, Oberkochen, Germany), each hemisphere of the cortices was separated from the midbrain and the meninges were peeled away from the cortex. All procedures were performed in 35-mm cell culture dishes (SPL Life Sciences, Pocheon, South Korea) filled with HBSS. Isolated cortexes were dissected into smaller pieces and the cortex pieces were transferred to a 50 mL conical tube filled with HBSS. Next, 3 mL of 0.25% trypsin-ethylenediaminetetraacetic acid was added to the dissected cortex and the mixture was incubated in a water bath at 37°C for 30 min. After incubation, the cell pellet was collected by centrifugation at 1,500*g* for 5 min and the pellet was suspended in DMEM containing 10% FBS and, 1% antibiotics and seeded in a 75 T flask. The flask was incubated at 37°C in a 5% CO_2 incubator. The media was replaced every 3 days. After 7–8 days, when the cell densities reached 100%, microglia and oligodendrocytes were removed from the mixed cortical culture. To isolate astrocytes from the microglia and oligodendrocytes, the flasks were placed on a rotary shaker at 180 rpm for 30 min to detach the microglia. After the medium was replaced and the unattached microglial cells were removed, the flask was vigorously shaken at 250 rpm for 6 h to detach the oligodendrocytes. The media was discarded and the remaining astrocytes were trypsinized. Isolated astrocytes were pelleted by centrifugation, re-suspended in growth medium, and seeded in a new 75T flask. The medium was replaced every 3 days till 14 days after astrocyte isolation. After 14 days, the cells were detached and seeded on 6-well plates with 5×10^5 cells/well for further experimentation.

3-(4,5-dimethylthiazol-2-yl)-2,5-diphenyl tetrazolium bromide (MTT) tetrazolium reduction assay

An MTT tetrazolium reduction assay was used to determine cell viability. Cells were seeded into 96-well plates at 8,000 cells/well. After 24 h, cells were treated with the indicated concentrations of $CoCl_2$ or subjected to the hypoxic gas mixture for the indicated time. After treatment, 20 μL of thiazolyl blue tetrazolium bromide solution (5 mg/mL) was added to each well and cells were incubated for 1 h at 37°C in the dark. The optical density at 540 nm was then measured with an EL800 microplate reader (Biotek Instruments, Winooski, VT, USA).

Caspase-1 activity assay

The activity of caspase-1 in T98G cells and primary astrocytes was measured using a caspase activity assay kit (BioVision Inc., Mountain View, CA, USA), following the manufacturer's instructions. The optical density of the

sample at 405 nm was monitored using an EL800 microplate reader (Biotek Instruments).

Western blotting analysis

Treated cells were harvested and lysed in cold PRO-PREP™ protein extraction solution (Intron Biotechnology, Seoul, South Korea). The lysates were centrifuged at 20,000*g* for 6 min at 4°C. The supernatant was collected and proteins were quantified using the Bradford protein assay (Bio-Rad, Hercules, CA, USA). Proteins were mixed with 5× protein sample buffer (ELPIS BIOTECH, Daejeon, South Korea) and boiled. Protein samples (10–80 μg) were size-separated by 7.5–15% sodium dodecyl sulfate polyacrylamide gel electrophoresis and transferred to a nitrocellulose membrane (PALL Life Sciences, East Hill, NY, USA). The membrane was blocked with 5% (w/v) skim milk (Santa Cruz Biotechnology, Dallas, TX) in 1× Tris-buffered saline (1 mM Tris, 150 mM NaCl, 0.1% Tween20, pH 7.4) for 1 h at room temperature. The blocked membrane was incubated with primary antibodies overnight at 4°C. The primary antibodies included anti-glyceraldehyde 3-phosphate dehydrogenase (GAPDH), anti-PARP, anti-cleaved caspase-3, anti-cleaved caspase-7, anti-caspase-8, and anti-cleaved caspase-9 antibodies from Cell Signaling Technology (Danvers, MA, USA); anti-Dicer, anti-β-actin antibodies from Santa Cruz Biotechnology; and anti-cleaved caspase-1 antibody from Abcam (Cambridge, UK). After being washed, each immunoblot was incubated with an appropriate horseradish peroxidase-labeled secondary antibody (Cell Signaling Technology) and visualized using an enhanced chemiluminescence kit (Advansta Inc., Menlo Park, CA, USA), and X-ray film (AGPA, Mortsel, Belgium). GAPDH and β-actin were used as an internal control.

Reactive oxygen species (ROS) assay

Cells were seeded onto a 12-mm round coverslip (Marlenfeld GmbH & Co., Lauda-Könlgshofen, Germany) and treated with $CoCl_2$ or subjected to the hypoxic gas mixture. The cell culture medium was changed to 10 μM DCF-DA (H2DCFDA) and cells were incubated at 37°C for 30 min in the dark. After discarding the DCF-DA working solution, the cells were incubated with Hoechst 33342 for 5 min. After washing, the coverslips were inverted and mounted on glass slides with mounting solution (glycerol:phosphate-buffered saline = 9:1). Images were captured using a fluorescence microscope (BX 51 optical system microscope; Olympus, Tokyo, Japan) equipped with an Olympus DP72 camera and the standard Cellsense program (Olympus). DCF-DA images were analyzed using ImageJ (NIH, Bethesda, MD, USA) to calculate the average background-corrected intensity.

Antisense oligonucleotide transfection

One day before transfection, T98G cells were plated at a density of 1×10^5 cells/well in a 12-well plate. After 24 h, the oligonucleotides complexed with Lipofectamine™ 2000 (Invitrogen, Carlsbad, CA, USA) were delivered into the cells. At the time of transfection, 150 μL of the mixture was added to each well (final concentration: 0.7 μM of oligonucleotide). After 24 h, the transfection medium was replaced with fresh DMEM, and the cells were harvested after 48 h. The sequences of the oligonucleotides were as follows: antisense control, 5′-TTG GTA ATA CGT GTT GAC TGT GA -3′ and antisense Dicer, 5′-GCU GAC CTT TTT GCT TCT CA-3′ (Tarallo et al., 2012) (Integrated DNA Technologies, Inc., Coralville, IA, USA)

Statistical analysis

Statistical analysis was performed using GraphPad Prism 5 (GraphPad Software Inc., San Diego, CA, USA). All experiments were performed at least three times. A Student's *t* test was used to compare two sets of data. For the analysis of multiple datasets, a one-way analysis of variance was used with variance and a post hoc Dunnett's test. Values are shown as mean ± standard error of the mean. Differences were considered to be statistically significant when $^*P < 0.05$, $^{**}P < 0.01$, $^{***}P < 0.005$.

Results

Hypoxia decreases the viability of astrocytes through caspase-3-dependent apoptosis

During hypoxia, HIF-1α accumulates in the nucleus of cells and activates several adaptive responses. Cobalt (II) chloride hexahydrate ($CoCl_2 \cdot 6H_2O$, MW = 237.9), which is known to induce HIF-1α accumulation, was used to mimic hypoxic conditions (Wu and Yotnda, 2011). Hypoxia-induced astrocyte death has previously been reported (Bondarenko and Chesler, 2001), but the detailed mechanism is not fully understood. To investigate whether hypoxia alters astrocyte viability, the viability of $CoCl_2$-treated human glioblastoma T98G cells was examined. Cell viability gradually decreased in a dose- and time-dependent manner following $CoCl_2$ treatment (Figures 1A and 1B). In addition to $CoCl_2$-induced chemical hypoxia, T98G cells were ventilated with a hypoxic gas mixture (1% O_2, 5% CO_2, and 94% N_2) for the indicated time to create a hypoxic environment. Cell viability decreased after 24 h of hypoxia (Figure 1C). Primary astrocytes were isolated from a mouse mixed cortical culture. Primary astrocytes were also treated with $CoCl_2$, which resulted in a gradual dose-dependent decrease in cell viability (Figure 1D). Therefore,

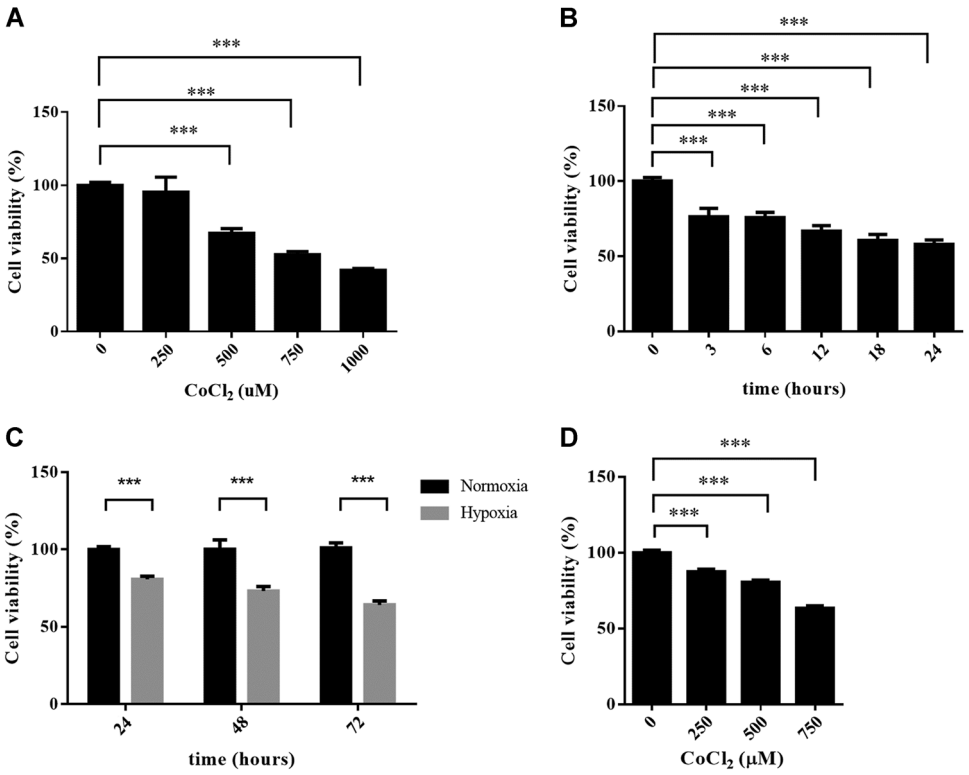

Figure 1 Hypoxia reduced the viability of astrocytes. (A) T98G cells were treated with the indicated doses of $CoCl_2$ (0, 250, 500, 750, and 1,000 μM) for 24 h. Cell viability was measured using an MTT tetrazolium reduction assay. The untreated control cells from three separate experiments were set as 100% ($n = 3$). (B) T98G cells treated with 750 μM of $CoCl_2$ for the indicated periods of time (0, 3, 6, 12, 18, and 24 h). The number of viable cells was measured by an MTT tetrazolium reduction assay. The number of untreated viable cells was set as 100%. Data represent the mean ± SEM of three independent experiments. Data were analyzed by one-way ANOVA, followed by Dunnet's post hoc test. ***$P < 0.005$ ($n = 3$). (C) The cell viability was measured by an MTT tetrazolium reduction assay. T98G cells were incubated in a humidified 37°C H35 hypoxystation at 1% O_2 for the indicated time points. The normoxia control group was set as 100%. Data represent the mean ± SEM of three independent experiments. Data were analyzed by Student's *t* test. ***$P < 0.005$ ($n = 3$). (D) Primary astrocytes were treated with the indicated doses (0, 250, 500, and 750 μM) of $CoCl_2$ for 48 h. Cell viability was measured using an MTT tetrazolium reduction assay. Data represent the mean ± SEM of three independent experiments. Data were analyzed by one-way ANOVA followed by Dunnet's post hoc test. ***$P < 0.005$ ($n = 3$). ANOVA, analysis of variance; MTT, 3-(4,5-dimethylthiazol-2-yl)-2,5-diphenyl tetrazolium bromide; SEM, standard error of the mean.

we confirmed that hypoxia reduced the number of viable astrocytes in vitro.

To determine the mechanisms involved in reduced astrocyte viability during hypoxia, apoptosis-associated proteins were examined. T98G cells were exposed to the indicated doses of $CoCl_2$ for the indicated time and the level of poly (ADP-ribose) polymerase (PARP) protein was examined by western blotting analysis using an anti-PARP antibody. Cleavage of PARP was detected after 12 h of treatment with 750 μM $CoCl_2$ (Figures 2A and 2B). During apoptosis, PARP is cleaved by executioner caspases, such as caspase-3 and -7 (Villa et al., 1997). It is well-established that caspase-8 and -9 are upstream of caspase-3 and -7 (Stennicke et al., 1998). Therefore, to determine whether caspase-3 and -7 are involved in the $CoCl_2$-induced apoptosis of T98G cells, the cleavage of caspase-3, -7, -8, and -9 were assessed. The levels of cleaved caspase-3, -7, -8, and -9 were increased by $CoCl_2$ in a dose- and time-dependent manner. Apoptosis was induced through the classical caspase-dependent apoptotic pathway in $CoCl_2$-treated T98G human glioblastoma cells. In addition, T98G cells were ventilated with a hypoxic gas mixture (1% O_2, 5% CO_2, and 94% N_2) for the indicated duration to create a hypoxic environment. PARP was cleaved after 48 h of incubation in the hypoxic gas (Figure 2C). After 72 h of incubation post seeding, minor PARP cleavage was seen in the normoxia group, but there was a significant increase in PARP cleavage during hypoxic gas incubation. In addition, primary astrocytes were treated with $CoCl_2$. PARP was also cleaved in primary astrocytes during chemical hypoxia (Figure 2D). These results indicated that hypoxia-induced the caspase-3-dependent apoptosis of astrocytes.

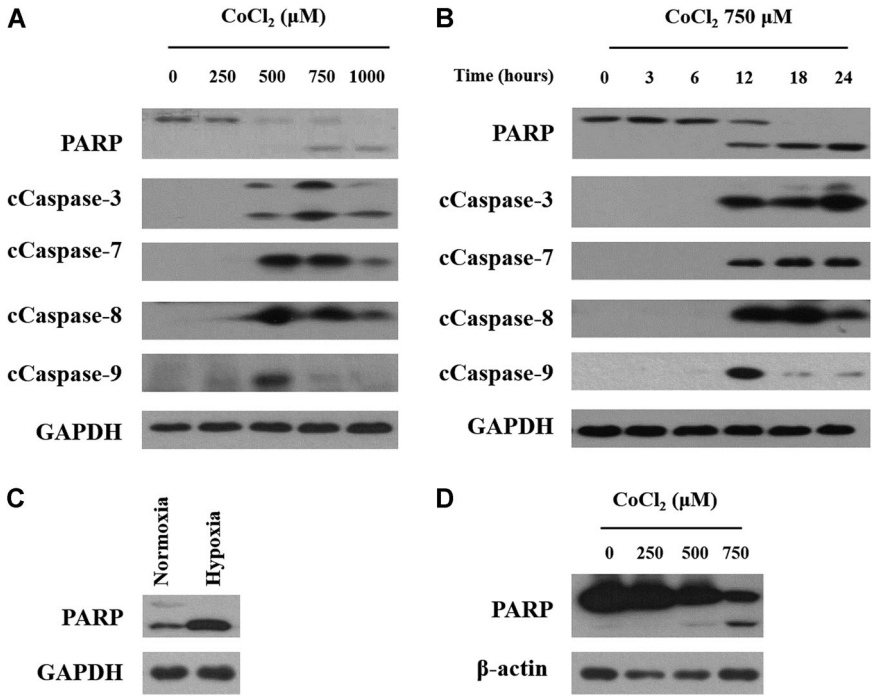

Figure 2 $CoCl_2$-mediated chemical hypoxia-induced apoptosis via the classical caspase-3-dependent pathway in T98G cells. (A) T98G cells were treated with the indicated doses (0, 250, 500, 750, and 1,000 μM) of $CoCl_2$ for 24 h ($n = 3$). (B) T98G cells were treated with 750 μM $CoCl_2$ for the indicated periods of time (0, 3, 6, 12, 18, and 24 h). PARP, cleaved caspase-3 (cCaspase-3), cleaved caspase-7 (cCaspase-7), cleaved caspase-8 (cCaspase-8), and cleaved caspase-9 (cCaspase-9) were analyzed by western blotting. GAPDH was used as an internal control ($n = 3$). (C) T98G cells were incubated in a humidified H35 hypoxystation at 37°C with 1% O_2 for 48 h. Western blotting analysis was performed using an anti-PARP antibody. GAPDH was used as an internal control ($n = 3$). (D) Primary astrocytes were treated with the indicated doses (0, 250, 500, and 750 μM) of $CoCl_2$ for 48 h. Western blotting analysis was performed using an anti-PARP antibody. Each experiment was performed at least three times. β-Actin was used as an internal control ($n = 3$). GAPDH, glyceraldehyde 3-phosphate dehydrogenase; PARP, poly (ADP-ribose) polymerase.

Caspase-1 is involved in the hypoxia-induced apoptosis of astrocytes

It has been reported that caspase-1, which is mainly known for mediating pyroptotic cell death, can also induce caspase-3-dependent apoptosis (Krishnamoorthy et al., 1999). Therefore, further experiments were performed to test whether caspase-1 is activated and participates in apoptosis during T98G cell hypoxia. Activation of caspase-1 was verified by western blotting and caspase-1 activity assays. Cleaved caspase-1 levels and caspase-1 activity were increased by $CoCl_2$ in a time-dependent manner (Figures 3A and 3B). Cleaved caspase-1 levels and caspase-1 activity also increased in T98G cells exposed to the hypoxic gas mixture (Figures 3C and 3D) and $CoCl_2$-treated primary astrocytes (Figures 3E and 3F). These results indicated that caspase-1 is activated in astrocytes during hypoxia.

To determine whether the activation of caspase-1 was involved in T98G cell death during hypoxia, an experiment was performed using the specific caspase-1 inhibitor (Ac-YVAD-CMK). T98G cells were treated with $CoCl_2$ in the presence or absence of the caspase-1 inhibitor for 24 h. As shown in Figure 3G, treatment with 100 μM Ac-YVAD-CMK resulted in a decrease in the levels of cleaved caspase-3, -7, -8, -9, and PARP during chemical hypoxia. Taken together, these results suggested that caspase-1 was activated during hypoxia and was involved in classical caspase-dependent apoptosis in astrocytes.

ROS activate caspase-1 during hypoxia in astrocytes

Previous studies have demonstrated that during hypoxia, ROS are generated in the pulmonary vasculature (Paddenberg et al., 2003), skeletal muscle (Clanton, 2007), and glioblastoma (Hsieh et al., 2012). To determine whether T98G cells generated ROS during $CoCl_2$ treatment, an ROS assay was performed. 2′,7′-dichlorofluorescin diacetate is a fluorogenic dye that reacts with ROS to generate a green fluorescent signal. A greater proportion of $CoCl_2$-treated T98G cells than untreated control cells were positive for DCF-DA (Figure 4A).

ROS plays a dual role in apoptosis (Simon et al., 2000). To determine whether hypoxia-induced apoptosis was related to the overproduction of ROS, cells were co-treated with $CoCl_2$ and the antioxidant, *N*-acetyl-cysteine (NAC). The viability of T98G cells treated with 750 μM

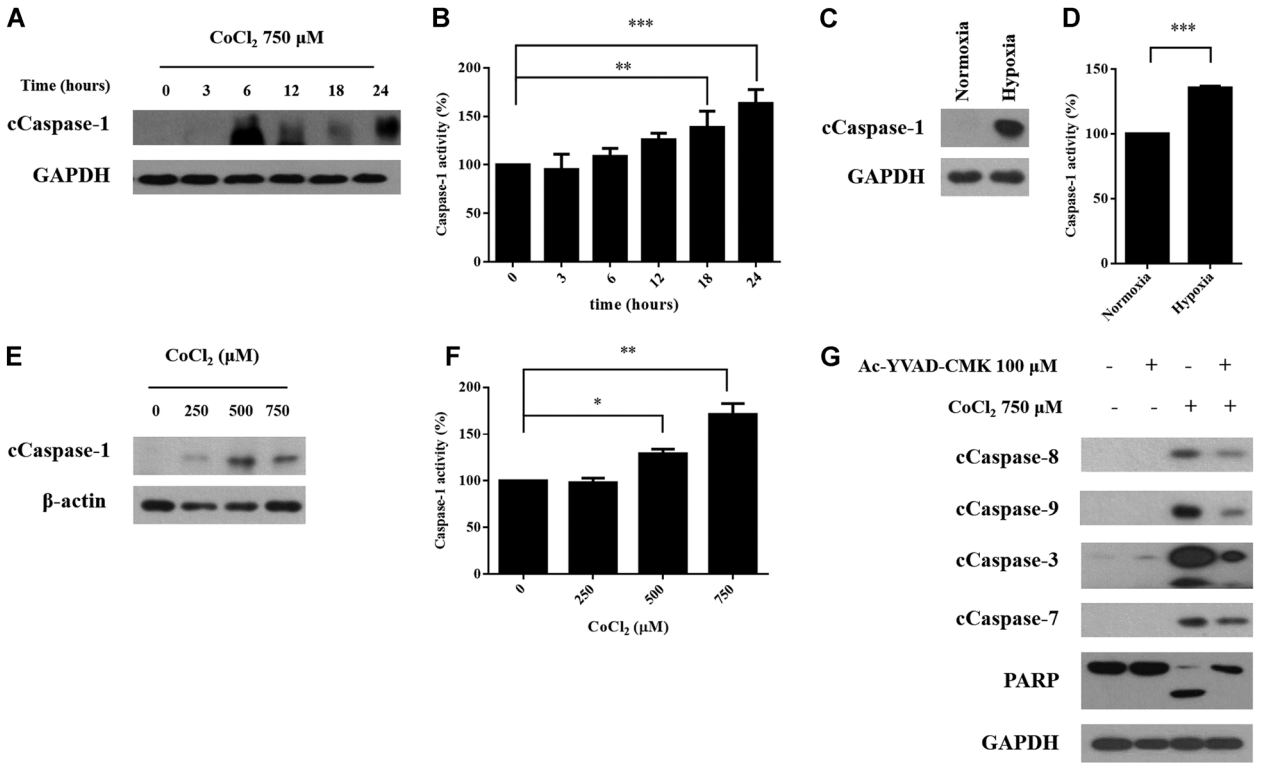

Figure 3 Activation of caspase-1 during hypoxia-induced apoptosis of T98G cells. (A and B) T98G cells were treated with 750 μM $CoCl_2$ for the indicated periods of time (0, 3, 6, 12, 18, and 24 h). (A) Activated caspase-1 was detected by western blotting analysis using an anti-cleaved caspase-1(cCaspase-1) antibody and (B) the activity of caspase-1 was measured using a caspase-1 activity assay. Each experiment was performed at least three times. Data were analyzed by one-way ANOVA followed by Dunnet's post hoc test. $^{**}P < 0.01$, $^{***}P < 0.005$ ($n = 3$). (C and D) T98G cells were incubated in a H35 hypoxystation at 37°C with a humidified 1% O_2 atmosphere for 48 h. (C) Activated caspase-1 was detected by western blotting analysis using an anti-cCaspase-1 antibody and (D) caspase-1 activity was measured using a caspase-1 activity assay. The absorbance of the untreated control group was set as 100%. Data were analyzed by Student's *t* test. $^{***}P < 0.005$ ($n = 3$). (E and F) Primary astrocytes were treated with the indicated doses (0, 250, 500, and 750 μM) of $CoCl_2$ for 48 h. (E) Activated caspase-1 was detected by western blotting analysis using an anti-cCaspase-1 antibody and (F) the activity of caspase-1 was measured using a caspase-1 activity assay. Data were analyzed by one-way ANOVA followed by Dunnet's post hoc test. $^{*}P < 0.05$, $^{**}P < 0.01$ ($n = 3$). (G) T98G cells were treated with 750 μM $CoCl_2$, with or without 100 μM caspase-1 specific inhibitor (Ac-YVAD-CMK) for 24 h. Cells were pre-treated with Ac-YVAD-CMK for 2 h prior to $CoCl_2$ treatment. Western blotting analysis was performed using anti-caspase-8, -cCaspase-9, -cCaspase-3, -cCaspase-7, and -PARP antibodies. GAPDH was used as an internal control ($n = 3$). ANOVA, analysis of variance; GAPDH, glyceraldehyde 3-phosphate dehydrogenase.

$CoCl_2$ was recovered in a concentration-dependent manner upon co-treatment with NAC (Figure 4B). In addition, treatment with NAC (5 mM) decreased $CoCl_2$-induced cleavage of caspase-3, -7, -8, -9, and PARP and the upstream caspase-1. ROS can also act as a common upstream activator of caspase-1 (Sorbara and Girardin, 2011) (Figures 4C–E). Taken together, these results suggested that ROS are an upstream signal of the apoptotic caspases during T98G cell death due to chemical-induced hypoxia.

Dicer is downregulated during hypoxia and knockdown of Dicer triggers apoptosis in astrocytes

Dicer is a miRNA-processing enzyme required for the maturation of miRNAs. Previous studies have reported that Dicer is downregulated under hypoxic conditions (Rupaimoole et al., 2014). Western blotting analysis was performed to determine whether chemical hypoxia reduces Dicer protein expression in astrocytes. Dicer protein levels were reduced by $CoCl_2$ in a dose- and time-dependent manner (Figures 5A and 5B). There was also a decrease in Dicer protein levels after incubation with the hypoxic gas mixture for 48 h (Figure 5C). A similar result was obtained in $CoCl_2$-treated primary astrocytes (Figure 5D). As a result, the level of Dicer protein was significantly reduced in astrocytes during hypoxia. On the basis of previous reports, the apoptotic machinery appears to be implicated in the regulation of Dicer. Active caspase-3 cleaves Dicer into a truncated form and truncated Dicer (tDicer) triggers cell death (Mosca et al., 2015). Western blotting analysis was performed to determine whether the decrease in Dicer levels

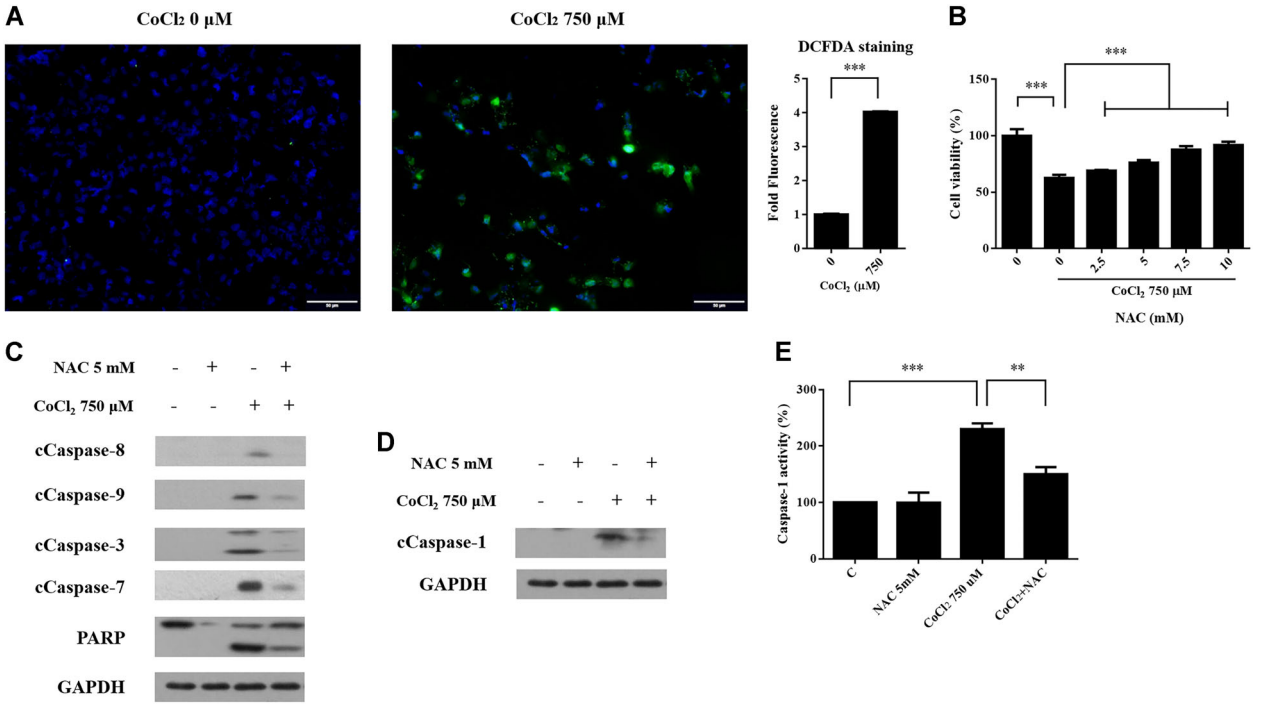

Figure 4 Decreased hypoxia-induced apoptosis in T98G cells by ROS scavenging. (A) T98G cells were treated with 750 μM $CoCl_2$ for 24 h. The effect of $CoCl_2$ on ROS generation was determined using a 2′,7′-dichlorofluorescin diacetate (DCF-DA) assay, visualized with a fluorescence microscope. Images were captured from random fields (magnification, ×200). Data are representative images of each condition from three separate experiments. (B) Cells were treated with 750 μM $CoCl_2$ in the presence or absence of the indicated dose (0, 2.5, 5, 7.5, 10 mM) of *N*-acetyl-cysteine (NAC) for 24 h. Cell viability was measured using an MTT tetrazolium reduction assay. The viability of the untreated control group was set as 100%. Each experiment was performed at least three times. Data were analyzed by one-way ANOVA followed by Dunnet's post hoc test. $***P < 0.005$ ($n = 3$). (C) T98G cells were treated with 750 μM $CoCl_2$ in the presence or absence of 5 mM NAC for 24 h. Cleaved caspase-8, -9, -3, -7, and -PARP were assessed by western blotting analysis using specific antibodies ($n = 3$). (D) Active caspase-1 was assessed by western blotting analysis using an anti-cCaspase-1 antibody ($n = 3$). (E) The activity of caspase-1 was measured using a caspase-1 activity assay, using the caspase-1 substrate, AC-VAD-pNA. The absorbance of the untreated control group was set as 100%. Each condition consisted of cells from three separate experiments. Data were analyzed by Student's *t* test. $**P < 0.01$, $***P < 0.005$ ($n = 3$). ANOVA, analysis of variance; MTT, 3-(4,5-dimethylthiazol-2-yl)-2,5-diphenyl tetrazolium bromide; ROS, reactive oxygen species.

was due to cleavage. tDicer contains the C-terminal region and can be detected using an anti-Dicer antibody. tDicer was increased 12 h after $CoCl_2$ treatment (Figure 5E). Experiments using a specific caspase-3/7 inhibitor (Z-DEVD-FMK) were then performed to further confirm that the truncation of Dicer was caused by active caspase-3. As shown in Figure 5F, Z-DEVD-FMK pre-treatment prevented the decrease in Dicer levels in $CoCl_2$-treated T98G cells.

To further verify the role of Dicer, antisense oligonucleotide (ASO)-induced protein knockdown was performed. Dicer expression levels were reduced in Dicer ASO-transfected cells compared with control ASO-transfected cells (Figure 6A). The viability of Dicer ASO-transfected cells was also reduced and was less than 65% of control ASO-transfected cell viability (Figure 6B). Western blotting analysis was performed to determine whether the knockdown of Dicer triggered T98G cell apoptosis. Cleaved caspase-3, -7, -8, -9, and PARP were detected in Dicer-knockdown cells (Figure 6C). Taken together, these results suggested that the caspase-dependent apoptotic pathway was activated in Dicer-knockdown T98G cells.

As shown in Figures 3 and 4, the ROS/caspase-1 pathway activated caspase-3-dependent apoptosis during hypoxia in astrocytes. These results suggest that the decrease in Dicer levels may also be involved in ROS/caspase-1 activation. Therefore, western blotting analysis and caspase-1 activity assays were performed to determine whether apoptosis induced by decrease in Dicer levels occurred via caspase-1 activation. Dicer-knockdown cells had increased levels of active caspase-1 (p20) compared with control ASO-transfected cells (Figure 6D). In addition, an ROS assay was used to determine whether caspase-1 activity was increased in Dicer ASO-transfected T98G cells (Figure 6E). Analysis of ROS generation by visualizing DCF-DA fluorescence with a fluorescence microscope showed that the knockdown of Dicer resulted in ROS generation in T98G cells (Figure 6F).

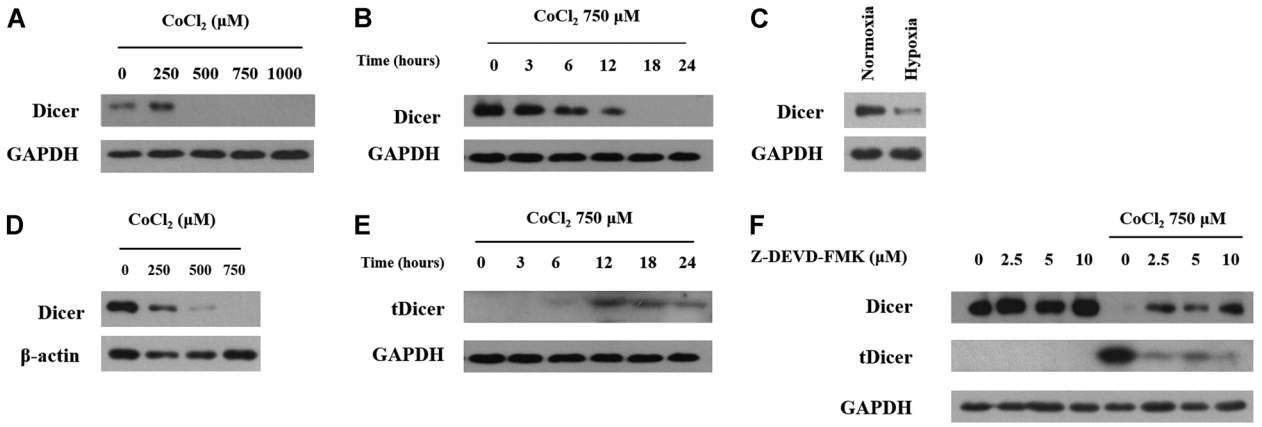

Figure 5 Downregulated Dicer expression during hypoxia-induced astrocyte apoptosis. (A) T98G cells were treated with the indicated concentrations of $CoCl_2$ (0, 250, 500, 750, and 1,000 μM) for 24 h. Dicer was detected by western blotting analysis using an anti-Dicer antibody ($n = 3$). (B) T98G cells were treated with $CoCl_2$ (750 μM) for the indicated periods of time (0, 3, 6, 12, 18, and 24 h). The protein level of Dicer was assessed by western blotting analysis using an anti-Dicer antibody. GAPDH was used as an internal control ($n = 3$). (C) T98G cells were incubated in a humidified H35 hypoxystation at 37°C with 1% O_2 for 48 h ($n = 3$). (D) Primary astrocytes were treated with the indicated doses (0, 250, 500, and 750 μM) of $CoCl_2$ for 48 h. The protein level of Dicer was assessed by western blotting analysis using an anti-Dicer antibody. Each experiment was performed at least three times. β-Actin was used as an internal control for primary astrocytes ($n = 3$). (E) T98G cells were treated with $CoCl_2$ (750 μM) for the indicated periods of time (0, 3, 6, 12, 18, and 24 h). The protein level of truncated Dicer (tDicer) was assessed by western blotting analysis using an anti-Dicer antibody ($n = 3$). (F) T98G cells were treated with 750 μM of $CoCl_2$ for 24 h. Two hours prior to $CoCl_2$ treatment, the indicated concentrations of a caspase-3/7 specific inhibitor (Z-DEVD-FMK; 0, 2.5, 5, and 10 μM) were added. Western blotting analysis was used to detect Dicer and tDicer using an anti-Dicer antibody. Data are representative images of cells from three separate experiments for each condition ($n = 3$). GAPDH, glyceraldehyde 3-phosphate dehydrogenase.

In conclusion, the downregulation of Dicer triggered caspase-dependent apoptosis via ROS generation and caspase-1 activation. Moreover, hypoxia-induced apoptosis was further reinforced by a positive feedback loop, in which caspase-3 decreased Dicer levels, while this decrease in Dicer levels resulted in ROS generation, which activated caspase-dependent apoptosis. Such a positive feedback loop may amplify the hypoxia-induced apoptosis of astrocytes.

Discussion

Hypoxia is a condition in which the whole body or a region of the body is deprived of oxygen supply. The organs most affected by hypoxia are the brain, heart, and liver (Erecińska and Silver, 2001). Cerebral hypoxia in particular can rapidly cause severe brain damage and even death (Vannucci, 1990). The protection of astrocytes against hypoxic damage is a promising therapeutic strategy (Zhao and Rempe, 2010). However, the mechanism of hypoxia-induced astrocyte death is not yet fully understood. In this study, we investigated the mechanism of astrocyte death during chemical hypoxia and examined the link between hypoxia-induced apoptosis and the RNase, Dicer. As shown in Figures 1C and 2C, hypoxic gas incubation for 48 hours decreased the viability of cells and increased the levels of cleaved PARP. After 72 h of incubation post seeding, minor PARP cleavage was observed in the normoxia group, but there was a significant increase in PARP cleavage during hypoxic gas incubation.

The downregulation of Dicer by post-translational cleavage has previously been reported. Caspase-3, a major executioner caspase during apoptosis, cleaves and converts Dicer to a death-promoting deoxyribonuclease (Nakagawa et al., 2010). For the first time, we found that astrocyte death during hypoxia is mediated by the ROS/caspase-1/classical caspase-dependent apoptotic pathway and the decrease in Dicer levels due to its cleavage by active caspase-3. This amplifies the apoptotic pathway through a positive feedback loop. These findings may provide a new target for therapeutic intervention in cerebral hypoxia.

It has become clear that astrocytes have an important function in the restoration of injured brain tissues. Considering that one of the main functions of astrocytes is to maintain extracellular ion concentrations for neurons, astrocytes have a significant role in neuronal damage control during brain damage (Sofroniew and Vinters, 2010). Under hypoxic conditions, astrocytes secrete neuroprotective factors, such as VEGF and erythropoietin to protect neurons from death (Jin et al., 2002). Therefore, preventing astrocyte death remains a potential therapeutic intervention strategy.

The classical caspase-dependent apoptotic pathway is dependent on caspase-3 (Villa et al., 1997). The classical caspase-dependent pathway participates in apoptosis

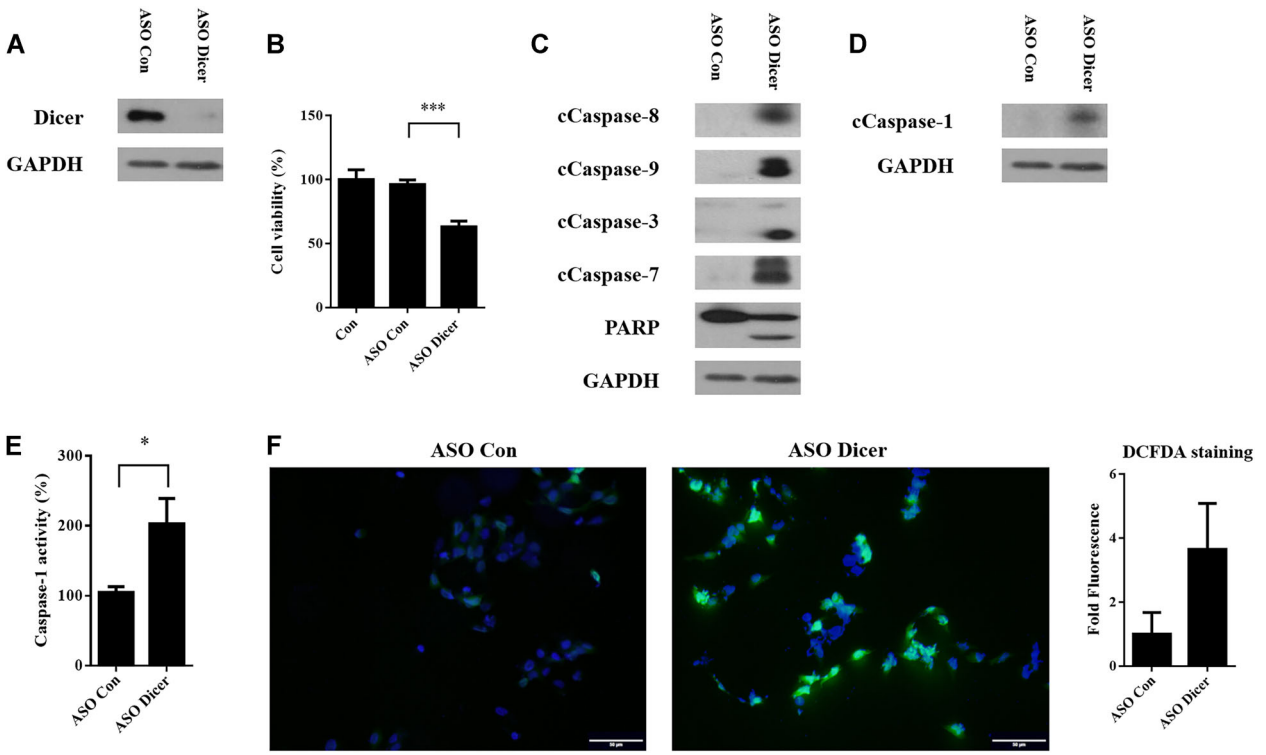

Figure 6 Apoptosis via the classical caspase-dependent pathway by Dicer knockdown. ASO-mediated knockdown of Dicer was performed. (A) The knockdown efficiency of Dicer was confirmed by western blotting analysis using an anti-Dicer antibody. GAPDH was used as an internal control ($n = 3$). (B) The number of viable cells was determined using an MTT tetrazolium reduction assay. The cell viability of un-transfected cells was set as 100%. Each condition consisted of cells from three separate experiments. Data were analyzed by the Student's t test. $^{***}P < 0.005$ ($n = 3$). (C) After transfection, T98G cells were collected and western blotting analysis was performed to verify the activation of the caspase-dependent apoptotic pathway using anti-cCaspase-3, -cCaspase-7, -Caspase-8, -cCaspase-9, and -PARP antibodies. GAPDH was used as an internal control ($n = 3$). (D) Active caspase-1 was analyzed by western blotting using an anti-cCaspase-1 antibody. GAPDH was used as an internal control ($n = 3$). (E) Caspase-1 activity was measured using a caspase-1 activity assay. The absorbance of the control ASO-transfected cells was set as 100%. Data represent the mean ± SEM of three independent experiments. Data were analyzed by Student's t test. $^{*}P < 0.05$ ($n = 3$). (F) The effect of Dicer knockdown on ROS generation was determined using a DCF-DA assay, visualized with a fluorescence microscope. Images were captured from random fields (magnification, ×200; $n = 3$). ASO, antisense oligonucleotide; DCF-DA, 2′,7′-dichlorofluorescin diacetate; GAPDH, glyceraldehyde 3-phosphate dehydrogenase; MTT, 3-(4,5-dimethylthiazol-2-yl)-2,5-diphenyl tetrazolium bromide; PARP, poly(ADP-ribose) polymerase; ROS, reactive oxygen species; SEM, standard error of the mean.

during hypoxia-induced astrocyte death (Giffard and Swanson, 2005). In this study, we present the first report on the involvement of caspase-1 during hypoxia-induced astrocyte death. Previous studies have reported that hypoxic stress can activate caspase-1 in ischemic acute tubular necrosis (Melnikov et al., 2002) and myocardial ischemia (Merkle et al., 2007). Hypoxia has been shown to activate caspase-1 in neurons (Zhang et al., 2003) and microglia (Kim et al., 2003). However, previous studies have not reported the relationship between caspase-1 and hypoxia in astrocytes. In contrast, Kim et al. (2013) reported that $CoCl_2$-induced hypoxia ameliorated caspase-1 activation in a mixed glial cell culture.

According to the results of this study, the downregulation of Dicer induced ROS generation and also amplified hypoxia-induced astrocyte death. Dicer is a type III ribonuclease that processes pre-miRNA into miRNA (MacRae et al., 2006). As Dicer is a critical regulator of miRNA biogenesis, it is becoming increasingly implicated in the regulation of a variety of cellular processes outside of its endonuclease function (MacFarlane and Murphy, 2010). Therefore, the ROS/caspase-1/classical caspase-dependent apoptosis of astrocytes induced by Dicer knockdown may not be directly connected to hypoxia-induced apoptosis. Further experiments are required to confirm the positive feedback loop initiated by the downregulation of Dicer during the chemical hypoxia-induced apoptosis of astrocytes.

Increasing evidence continues to demonstrate the critical role of Dicer not only in the biogenesis of miRNA and small interfering RNA in the canonical RNA interference pathway but also in controlling the fate of many other small

RNA species (MacRae et al., 2006). There is also evidence to suggest that Dicer directly regulates cytokine levels (Asirvatham et al., 2008). The regulation of hypoxia-induced cytokine production may be the mechanism involved in the hypoxia-induced apoptosis of astrocytes, but further experiments are needed to test this hypothesis. Dicer is involved in autophagy and is required for autophagosome formation (Gibbings et al., 2012). Gibbings et al. suggested that the loss of Dicer causes defects in the autophagy-lysosomal pathway and enhanced cytotoxicity. Therefore, a hypoxia-induced autophagy defect may be another link between the hypoxia-induced downregulation of Dicer and astrocyte apoptosis.

The cleavage of Dicer in response to apoptotic stimuli was first reported in 2008 and a few years later, it was confirmed that caspase-3 cleaved Dicer during apoptosis (Matskevich and Moelling, 2008; Nakagawa et al., 2010). In addition, Nakagawa et al. suggested the possibility that a truncated fragment of Dicer itself acted as a nuclease and induced DNA fragmentation in *Caenorhabditis elegans*. In T98G cells, a truncated fragment of Dicer was found to be increased by $CoCl_2$ in a dose- and time-dependent manner. Therefore, whether hypoxia-induced astrocyte death is solely mediated by ROS/caspase-1/classical caspase-dependent apoptosis or involves other forms of programmed cell death requires further investigation.

Acknowledgment

This research was supported by funding from the National Research Foundation of Korea (NRF- 2015R1D1A3A01019515 and 2017R1A5A2015369).

References

Ambati J, Fowler BJ (2012) Mechanisms of age-related macular degeneration. Neuron 75(1): 26–39. https://doi.org/10.1016/j.neuron.2012.06.018

Asirvatham A, Magner W, Tomasi T (2008) miRNA regulation of cytokine genes. Cytokine 45(2): 58–69. https://doi.org/10.1016/j.cyto.2008.11.010

Bondarenko A, Chesler M (2001) Rapid astrocyte death induced by transient hypoxia, acidosis, and extracellular ion shifts. GLIA 34(2): 134–42. https://doi.org/10.1002/glia.1048

Clanton TL (2007) Hypoxia-induced reactive oxygen species formation in skeletal muscle. J Appl Physiol 102(6): 2379–88. https://doi.org/10.1152/japplphysiol.01298.2006

Erecińska M, Silver IA (2001) Tissue oxygen tension and brain sensitivity to hypoxia. Respir Physiol 128(3): 263–76. https://doi.org/10.1016/s0034-5687(01)00306-1

Ge X, Zhao X, Nakagawa A, Gong X, Skeen-Gaar RR, Shi Y, Gong H, Wang X, Xue D (2014) A novel mechanism underlies caspase-dependent conversion of the dicer ribonuclease into a deoxyribonuclease during apoptosis. Cell Res 24(2): 218–32. https://doi.org/10.1038/cr.2013.160

Gibbings D, Mostowy S, Jay F, Schwab Y, Cossart P, Voinnet O (2012) Selective autophagy degrades DICER and AGO2 and regulates miRNA activity. Nature Cell Biol 14(12): 1314–21. https://doi.org/10.1038/ncb3208

Giffard RG, Swanson RA (2005) Ischemia-induced programmed cell death in astrocytes. GLIA 50(4): 299–306. https://doi.org/10.1002/glia.20167

Hsieh C-H, Chang H-T, Shen W-C, Shyu W-C, Liu R-S (2012) Imaging the impact of Nox4 in cycling hypoxia-mediated U87 glioblastoma invasion and infiltration. Mol Imaging Biol 14(4): 489–99. https://doi.org/10.1007/s11307-011-0516-0

Jin K, Zhu Y, Sun Y, Mao XO, Xie L, Greenberg DA (2002) Vascular endothelial growth factor (VEGF) stimulates neurogenesis in vitro and in vivo. Proc Natl Acad Sci U S A 99(18): 11946–50. https://doi.org/10.1073/pnas.182296499

Kim E-H, Won J-H, Hwang I, Yu J-W (2013) Cobalt chloride-induced hypoxia ameliorates NLRP3-mediated caspase-1 activation in mixed glial cultures. Immune Netw 13(4): 141–7. https://doi.org/10.4110/in.2013.13.4.141

Kim N-G, Lee H, Son E, Kwon O-Y, Park J-Y, Park J-H, Cho G, Suk K (2003) Hypoxic induction of caspase-11/caspase-1/interleukin-1β in brain microglia. Mol Brain Res 114(2): 107–14. https://doi.org/10.1016/s0169-328x(03)00135-9

Krishnamoorthy RR, Crawford MJ, Chaturvedi MM, Jain SK, Aggarwal BB, Al-Ubaidi MR, Agarwal N (1999) Photo-oxidative stress down-modulates the activity of nuclear factor-κB via involvement of caspase-1, leading to apoptosis of photoreceptor cells. J Biol Chem 274(6): 3734–43. https://doi.org/10.1074/jbc.274.6.3734

Kumar MS, Pester RE, Chen CY, Lane K, Chin C, Lu J, Kirsch DG, Golub TR, Jacks T (2009) Dicer1 functions as a haploinsufficient tumor suppressor. Genes Dev 23(23): 2700–4. https://doi.org/10.1101/gad.1848209

MacFarlane L-A, Murphy PR (2010) MicroRNA: biogenesis, function and role in cancer. Curr Genomics 11(7): 537–61. https://doi.org/10.2174/138920210793175895

MacRae IJ, Zhou K, Li F, Repic A, Brooks AN, Cande WZ, Adams PD, Doudna JA (2006) Structural basis for double-stranded RNA processing by Dicer. Science 311(5758): 195–8. https://doi.org/10.1126/science.1121638

Matskevich A, Moelling K (2008) Stimuli-dependent cleavage of Dicer during apoptosis. Biochem J 412(3): 527–34. https://doi.org/10.1042/bj20071461

Melnikov VY, Faubel S, Siegmund B, Lucia MS, Ljubanovic D, Edelstein CL (2002) Neutrophil-independent mechanisms of caspase-1–and IL-18–mediated ischemic acute tubular necrosis in mice. J Clin Invest 110(8): 1083–91. https://doi.org/10.1172/jci15623

Merkle S, Frantz S, Schön MP, Bauersachs J, Buitrago M, Frost RJ, Lohse SM, Engelhardt S (2007) A role for caspase-1 in heart failure. Circ Res 100(5): 645–53. https://doi.org/10.1161/01.res.0000260203.55077.61

Mosca N, Starega-Roslan J, Castiello F, Russo A, Krzyzosiak WJ, Potenza N (2015) Characterization of a naturally occurring truncated Dicer. Mol Biol Rep 42(8): 1333–40. https://doi.org/10.1007/s11033-015-3878-6

Nakagawa A, Shi Y, Kage-Nakadai E, Mitani S, Xue D (2010) Caspase-dependent conversion of Dicer ribonuclease into a death-promoting deoxyribonuclease. Science 328(5976): 327–34. https://doi.org/10.1126/science.1182374

Paddenberg R, Ishaq B, Goldenberg A, Faulhammer P, Rose F, Weissmann N, Braun-Dullaeus. RC, Kummer W (2003) Essential role of complex II of the respiratory chain in hypoxia-induced ROS generation in the pulmonary vasculature. Am J Physiol lung Cell Mol Physiol 284(5): L710–9. https://doi.org/10.1152/ajplung.00149.2002

Prabhakar NR (2001) Invited review: oxygen sensing during intermittent hypoxia: cellular and molecular mechanisms. J Appl Physiol 90(5): 1986–94. https://doi.org/10.1152/jappl.2001.90.5.1986

Rupaimoole R, Wu SY, Pradeep S, Ivan C, Pecot CV, Gharpure KM, Zand B (2014) Hypoxia-mediated downregulation of miRNA biogenesis promotes tumour progression. Nat Commun 5: 5202. https://doi.org/10.1038/ncomms6202

Salceda S, Caro J (1997) Hypoxia-inducible factor 1α (HIF-1α) protein is rapidly degraded by the ubiquitin-proteasome system under normoxic conditions Its stabilization by hypoxia depends on redox-induced changes. J Biol Chem 272(36): 22642–7. https://doi.org/10.1074/jbc.272.36.22642

Schildge S, Bohrer C, Beck K, Schachtrup C (2013) Isolation and culture of mouse cortical astrocytes. J Vis Exp 19(71): e50079. https://doi.org/10.3791/50079

Sendoel A, Hengartner MO (2014) Apoptotic cell death under hypoxia. Physiology 29(3): 168–76. https://doi.org/10.1152/physiol.00016.2013

Simon H-U, Haj-Yehia A, Levi-Schaffer F (2000) Role of reactive oxygen species (ROS) in apoptosis induction. Apoptosis 5(5): 415–8. https://doi.org/10.1023/a:1009616228304

Sofroniew MV, Vinters HV (2010) Astrocytes: biology and pathology. Acta Neuropathol 119(1): 7–35. https://doi.org/10.1007/s00401-009-0619-8

Sorbara MT, Girardin SE (2011) Mitochondrial ROS fuel the inflammasome. Cell Res 21(4): 558–60. https://doi.org/10.1038/cr.2011.20

Stennicke HR, Jürgensmeier JM, Shin H, Deveraux Q, Wolf BB, Yang X, Bredesen D (1998) Pro-caspase-3 is a major physiologic target of caspase-8. J Biol Chem 273(42): 27084–90. https://doi.org/10.1074/jbc.273.42.27084

Tarallo V, Hirano Y, Gelfand BD, Dridi S, Kerur N, Kim Y, Bogdanovich S (2012) DICER1 loss and Alu RNA induce age-related macular degeneration via the NLRP3 inflammasome and MyD88. Cell 149(4): 847–59. https://doi.org/10.1016/j.cell.2012.03.036

Vallés SL, Blanco AM, Pascual M, Guerri C (2004) Chronic ethanol treatment enhances inflammatory mediators and cell death in the brain and in astrocytes. Brain Pathol 14(4): 365–71. https://doi.org/10.1111/j.1750-3639.2004.tb00079.x

Vannucci RC (1990) Experimental biology of cerebral hypoxia-ischemia: relation to perinatal brain damage. Pediatr Res 27(4): 317–26. https://doi.org/10.1203/00006450-199004000-00001

Vieira H, Almeida A, Figueiredo-Pereira C, Queiroga C (2015) Carbon monoxide targeting mitochondria in astrocytes: modulation of cell metabolism, redox response and cell death. SpringerPlus 4(S1): L42. https://doi.org/10.1186/2193-1801-4-s1-l42

Villa P, Kaufmann SH, Earnshaw WC (1997) Caspases and caspase inhibitors. Trends Biochem Sci 22(10): 388–93. https://doi.org/10.1016/s0968-0004(97)01107-9

Wheaton WW, Chandel NS (2010) Hypoxia. 2. Hypoxia regulates cellular metabolism. Am J Physiol Cell Physiol 300(3): C385–93. https://doi.org/10.1152/ajpcell.00485.2010

Wu D, Yotnda P (2011) Induction and testing of hypoxia in cell culture. J Vis Exp 12(54): e2899. https://doi.org/10.3791/2899

Zhang W-H, Wang X, Narayanan M, Zhang Y, Huo C, Reed JC, Friedlander RM (2003) Fundamental role of the Rip2/caspase-1 pathway in hypoxia and ischemia-induced neuronal cell death. Proc Natl Acad Sci U S A 100(26): 16012–7. https://doi.org/10.1073/pnas.0308383101

Zhao Y, Rempe DA (2010) Targeting astrocytes for stroke therapy. Neurotherapeutics 7(4): 439–51. https://doi.org/10.1016/j.nurt.2010.07.004

Received 21 August 2019; accepted 1 March 2020.
Final version published online 12 March 2020.